

Three-particle cumulant Study of Conical Emission

Claude A. Pruneau

Physics and Astronomy Department, Wayne State University, Detroit, MI 48201 USA

We discuss the sensitivity of the three-particle azimuthal cumulant method for a search and study of conical emission in central relativistic $A + A$ collisions. Our study is based on a multicomponent Monte Carlo model which include flow background, Gaussian mono-jets, jet-flow, and Gaussian conical signals. We find the observation of conical emission is hindered by the presence of flow harmonics of fourth order (v_4) but remains feasible even in the presence of a substantial background. We consider the use of probability cumulants for the suppression of 2^{nd} order flow harmonics. We find that while probability cumulant significantly reduce v_2^2 contributions, they also complicate the cumulant of jets, and conical emission. The use of probability cumulants is therefore not particularly advantageous in searches for conical emission. We find the sensitivity of the (density) cumulant method depends inextricably on strengths of v_2 , v_4 , background and non-Poisson character of particle production. It thus cannot be expressed in a simple form, and without specific assumptions about the values of these parameters.

PACS numbers: 24.60.Ky, 25.75.-q, 25.75.Nq, 25.75.Gz

Keywords: Heavy ion collisions, three-particle azimuthal correlations, conical emission.

I. INTRODUCTION

Observations of away-side dip structures in two-particle correlations measured in $Au + Au$ collisions at $\sqrt{s_{NN}} = 200$ GeV have stimulated renewed interest in the notion of conical emission. The passage of a parton through dense matter at speeds greater than the speed of sound is predicted to lead to the production of a Mach shock wake resulting in conical emission pattern that may explain the observed two-particle correlations [1, 2, 3, 4, 5, 6, 7, 8, 9, 10, 11]. Identification of Mach cone is of great interest because it could provide an experimental determination of the speed of sound in the dense medium produced in high energy $A + A$ collisions [4, 12]. A sonic boom is also expected for a heavy quark propagation based on AdS/CFT calculation [13]. Cerenkov radiation produced by a superluminal parton traversing a dense medium is expected to generate a similar signature [14, 15, 16, 17, 18]. However, other production mechanisms have been proposed to explain the two-particle correlation data. These include large angle gluon radiation [19, 20], path length effects [21], collective flow, and jet deflection [22, 23, 24, 25, 26, 27].

Three-particle correlation measurements were proposed to gain further insight in the particle production mechanism leading to the away-side deep structure seen in two-particle correlations. Various methods have been suggested and are currently pursued to carry such analyses. A number of these analyses are carried out using a flow + signal decomposition, i.e. an adhoc flow background is assumed and subtracted based on the ZYAM approximation [28, 29, 30, 31, 32, 33, 34, 35, 36, 37, 38]. Note however that, as Borghini pointed out, momentum conservation can have a significant impact on two- and three-particle correlations [39]. The magnitude of momentum conservation effects is however difficult to estimate as discussed recently by Chajecski *et al.* [40]. A cumulant based method was proposed by the author [41] and is also used by the STAR collaboration [42] to search for conical emission. This method presents the advantage that the extraction of a three-particle signal does *not* require any model assumptions. Obviously, one can also carry a model based decomposition of the extracted three-particle signal, i.e. the cumulant, to estimate its various components, and seek evidence for conical emission.

In this work, we further study the properties of the three-particle cumulant observable first proposed in Ref. [41] for a search for conical emission, and studies of particle production dynamics. Three particles correlations, designed to search for conical emission, use a high p_t particle as a jet tag. The azimuthal angle of this high p_t particle should approximately correspond to the direction of the parton initiating the tagged jet. It is further assumed the emission of this parton is surface biased, and directed outward, approximately normal to the surface of the medium. The direction of the high- p_t particle thus provides a reference to study the propagation of the away-side parton initiating the second jet. Estimates of the sound velocity in the quark gluon plasma suggest the wake produced by a high energy parton should produce particle emission at a Mach angle of the order of one radian relative to the parton direction [4]. This corresponds to enhanced particle emission at angles of order 2 radian with respect to the high- p_t jet tag. An unsuppressed away-side jet should on the other hand lead to particle emission at an angle of approximately π relative to the jet tag. Deflection or radial flow effects should produce a broadening of the away-side jet relative to the high- p_t tag.

We define the notation and variables used in this paper in Section II. We next discuss, in Section III, simple models of particle production including di-jets, flow, conical emission, as well as the effects of differential jet quenching, hereafter called jet-flow. We show in Sec. III B that in the case of Poisson statistical particle production, the three particle cumulant (hereafter noted *3-cumulant*) associated with azimuthal anisotropy reduces to a simple expression involving only non-diagonal Fourier terms. In view of the large values of elliptic flow v_2 observed in $A + A$ collisions at RHIC, one expects the leading non-diagonal term should be of order $v_2 v_2 v_4$. However, one finds experimentally that fluctuations in the number of produced particles are non-Poissonian. We thus consider in Sec. IV the impact of such non-Poissonian fluctuations, and find they imply the presence of sizable v_2^2 terms in the three-cumulant that may complicate the observation of conical emission signals. We show the v_2^2 terms may however be suppressed if one adopts a modified version of the cumulant based on probability densities rather than number densities, and suggest this modified cumulant as an alternative means of studying three-particle correlations.

The cumulant method is a relatively complicated analysis technique, which may in principle be sensitive to various instrumental effects. We discuss a specific implementation of the method based on normalization to single particle distributions in Sec. V. We show, based on the conical emission model introduced in Sec. VI and an adhoc parameterization of the detection efficiency, that normalization by single particle distributions leads to a robust analysis technique.

A key issue in the search for conical emission is the sensitivity of the method used to extract the three-particle correlation information. We discuss, in Section VI, the sensitivity of the cumulant method based on a simple jet and conical emission Monte-Carlo model.

Our conclusions are summarized in Section VII.

II. DEFINITIONS AND NOTATION

The conical emission search method introduced in Ref. [41] is based on the observation of three-particle densities as a function of the relative azimuthal angles between the measured particles. The presence of three-particle correlations, and possible signal for conical emission is extracted using the *3-cumulants*. A high p_t particle is used as a jet tag, and proxy for determination of the direction of the jet. Two lower p_t particles are used to probe the structure of the near-side jet (i.e. the jet singled out by the high- p_t tag particle) and search for conical emission on the away-side. The jet tag is herein referred as particle 1 while the two associates are labeled as particles 2 and 3. The three particles are detected in the collision transverse plane at angles φ_1 , φ_2 , and φ_3 relative to some arbitrary reference frame. The single, two-, and three-particle densities are noted as follows:

$$\begin{aligned}\rho_1(\varphi_i) &= dN_1/d\varphi_i \\ \rho_2(\varphi_i, \varphi_j) &= dN_2/d\varphi_i d\varphi_j \\ \rho_3(\varphi_i, \varphi_j, \varphi_k) &= dN_3/d\varphi_i d\varphi_j d\varphi_k\end{aligned}\tag{1}$$

where the indices i , j , and k take values 1, 2, and 3.

The three-particle or triplet density, ρ_3 , corresponds to the average number of particle triplets observed per collision. The particles of a given triplet are however not necessarily correlated. Indeed, the three particles may originate from one, two, or three (distinct or not) production processes (e.g. radial flow, elliptic flow, resonance decay, jets, Mach cone, etc). Cumulants are designed to extract the three-particle correlation component from the three-particle density. They were first discussed in the context of particle physics (see for instance [43, 44]) and are now used in a variety of analyses. It is the purpose of this work to study specific aspects of the cumulant method introduced in [41] for studies of the shape and strength of the signal expected from different types of processes and to characterize the robustness and sensitivity of the method.

The 2- and 3-cumulants C_2 and C_3 are defined as follows:

$$\begin{aligned}C_2(\varphi_i, \varphi_j) &\equiv \rho_2(\varphi_i, \varphi_j) - \rho_1(\varphi_i)\rho_1(\varphi_j) \\ C_3(\varphi_i, \varphi_j, \varphi_k) &\equiv \rho_3(\varphi_i, \varphi_j, \varphi_k) - \rho_2(\varphi_i, \varphi_j)\rho_1(\varphi_k) \\ &\quad - \rho_2(\varphi_i, \varphi_k)\rho_1(\varphi_j) - \rho_2(\varphi_j, \varphi_k)\rho_1(\varphi_i) \\ &\quad + 2\rho_1(\varphi_i)\rho_1(\varphi_j)\rho_1(\varphi_k)\end{aligned}\tag{2}$$

As described in Ref. [41] the two-, three-particle densities and cumulants are straightforwardly corrected for detector inefficiencies provided the three- and two-particle detection efficiencies may be factorized as products of respectively two and three single particle efficiencies. The robustness of this correction procedure is discussed in Sec. V on the basis of Monte Carlo simulations.

Correlation functions in terms of relative angles, $C_3(\Delta\varphi_{ij}, \Delta\varphi_{ik})$, are formally obtained by integration of the cumulants $C_3(\varphi_i, \varphi_j, \varphi_k)$ with constraints $\Delta\varphi_{ij} = \varphi_i - \varphi_j$.

$$\begin{aligned} C_3(\Delta\varphi_{ij}, \Delta\varphi_{ik}) &= \int C_3(\varphi_i, \varphi_j, \varphi_k) \\ &\times \delta(\Delta\varphi_{ij} - \varphi_i + \varphi_j) \\ &\times \delta(\Delta\varphi_{ik} - \varphi_i + \varphi_k) d\varphi_i d\varphi_j d\varphi_k \end{aligned} \quad (3)$$

In practice, this is accomplished by binning $C_3(\varphi_i, \varphi_j, \varphi_k)$ and $C_3(\Delta\varphi_{ij}, \Delta\varphi_{ik})$ into arrays (e.g. 72x72x72 and 72x72 respectively) and summing the elements of $C_3(\varphi_i, \varphi_j, \varphi_k)$ to obtain $C_3(\Delta\varphi_{ij}, \Delta\varphi_{ik})$ as follows.

$$C_3(p, q) = \sum_{i,j,k=1}^{72} C_3(i, j, k) \delta(p - i + k) \delta(q - i + k) \quad (4)$$

for $p=1, \dots, 72$; $q=1, \dots, 72$. Given the finite statistics, and the large memory requirement implied by three-dimensional arrays used in this type of analysis, care must be taken when binning the densities. We found the use of 72 bins, for analysis of data samples collected e.g. by the STAR experiment [45, 46] enables sufficient angular resolution and statistical accuracy.

III. SIGNAL MODELING

We use specific models for jet, di-jet production, collective flow, and conical emission signals in order to assess the sensitivity of the cumulant method for a search of conical emission. The models are described in the following sub-sections while our study of the sensitivity of the cumulant method is presented in Section VI.

A. Di-Jet Production

Jet production is characterized by the emission of particles in a cone (in momentum space) centered on the direction of the parton that produces the jet. We consider di-jet production restricted to central rapidities (near 90° relative to the beam direction), and assume the number of di-jet per event in the acceptance of the detector, J , varies event-by-event. The intra-jet particle multiplicity depends on the jet energy, but is order three (3) at RHIC energy [47]. We consider back-to-back jets in azimuth, but possibly different longitudinal momenta. We denote the number of jet particles measured within each kinematics cut "i" as A_i and A'_i respectively for the near and away side jets. The emission of particles relative to the jet axis is described by a probability distribution $P_{assoc}(\theta)$, where θ is the angle between the particle momentum and the momentum vector of the parton originating the jet. Projection of this distribution in the transverse plane leads to a probability distribution, $P_J(\varphi)$, function of the azimuthal angle, φ , between the parton and the particle direction. Following [41], we further simplify the jet model and use a Gaussian azimuthal profile, $G_2(\varphi_i - \phi_\alpha; \sigma_i)$ with $G_2(x; \sigma) \equiv (\sqrt{2\pi}\sigma)^{-1} \exp(-x^2/2\sigma^2)$ where φ_i , ϕ_α , and σ_i are the emission angle (in the lab frame) of measured particles, the emission angle of the parton, and the width of the jet, respectively. For this illustrative model, we assume the emission angle and the jet multiplicity are not correlated to the collision reaction plane. We further assume one can decouple the number of particles, in the measured kinematic range of interest, from the jet profile. The number of jets, their multiplicity, and directions are not known, and must therefore be averaged out. The 3-particle jet cumulant is given by the following expression.

$$\begin{aligned} C_3^{Jet}(\Delta\varphi_{12}, \Delta\varphi_{13}) &= (2\pi)^{-1} \langle J \rangle \left\{ \begin{aligned} &\langle A_1 A_2 A_3 \rangle G_3(\Delta\varphi_{12}, \Delta\varphi_{13}; \sigma_1, \sigma_2, \sigma_3) \\ &+ \langle A_1 A_2 A'_3 \rangle G_3(\Delta\varphi_{12}, \Delta\varphi_{13} - \pi; \sigma_1, \sigma_2, \sigma'_3) \\ &+ \langle A_1 A'_2 A_3 \rangle G_3(\Delta\varphi_{12} - \pi, \Delta\varphi_{13}; \sigma_1, \sigma'_2, \sigma_3) \\ &+ \langle A_1 A'_2 A'_3 \rangle G_3(\Delta\varphi_{12} - \pi, \Delta\varphi_{13} - \pi; \sigma_1, \sigma'_2, \sigma'_3) \end{aligned} \right\} \\ &+ (2\pi)^{-2} \left(\langle J(J-1) \rangle - \langle J \rangle^2 \right) \left\{ \begin{aligned} &\langle A_1 A_2 \rangle \langle A_3 + A'_3 \rangle G_2(\Delta\varphi_{12}; \sigma_{12}) \\ &+ \langle A_1 A_3 \rangle \langle A_2 + A'_2 \rangle G_2(\Delta\varphi_{13}; \sigma_{13}) \\ &+ \langle A_2 A_3 \rangle \langle A_1 \rangle G_2(\Delta\varphi_{13} - \Delta\varphi_{12}; \sigma_{23}) \\ &+ \langle A_1 A'_2 \rangle \langle A_3 + A'_3 \rangle G_2(\Delta\varphi_{12} - \pi; \sigma'_{12}) \\ &+ \langle A_1 A'_3 \rangle \langle A_2 + A'_2 \rangle G_2(\Delta\varphi_{13} - \pi; \sigma'_{13}) \\ &+ \langle A'_2 A'_3 \rangle \langle A_1 \rangle G_2(\Delta\varphi_{13} - \Delta\varphi_{12}; \sigma'_{23}) \end{aligned} \right\} \\ &+ (2\pi)^{-3} \left(\langle J(J-1)(J-2) \rangle - 3 \langle J(J-1) \rangle \langle J \rangle + 2 \langle J \rangle^3 \right) \langle A_1 \rangle \langle A_2 + A'_2 \rangle \langle A_3 + A'_3 \rangle \end{aligned} \quad (5)$$

with

$$G_3(x_1, x_2; \sigma_1, \sigma_2, \sigma_3) = (2\pi)^{-1} \sigma_{1,2,3}^{-2} \times \exp\left(-(\sigma_3^2 x_1^2 + \sigma_2^2 x_2^2 + \sigma_1^2 (x_1 - x_2)^2) / 2\sigma_{1,2,3}^2\right) \quad (6)$$

where $x_{ij} = x_i - x_j$, $\sigma_{ij}^2 = \sigma_i^2 + \sigma_j^2$ and $\sigma_{i,j,k}^4 = \sigma_i^2 \sigma_j^2 + \sigma_i^2 \sigma_k^2 + \sigma_j^2 \sigma_k^2$. Note G_3 is defined such its integral over x_1 and x_2 is unity. The coefficient $\langle J \rangle$ determines the average number of jets per event. Coefficients A_1, A_2, A_3 describe the number of particles associated with the near side jet, while A'_1, A'_2, A'_3 correspond to the number of particles associated with the away side jet observed within the kinematic cuts used for the study of the correlation functions. We note that if the number of jets, J , in each event is determined by a Poisson process, then one has $\langle J(J-1) \rangle = \langle J \rangle^2$ and $\langle J(J-1)(J-2) \rangle - 3\langle J(J-1) \rangle - 2\langle J \rangle^3 = 0$. The constant term, and the terms containing a 2-particle dependence in G_2 then vanish in the above expression. The jet 3-cumulant is plotted in Figure 1, in arbitrary amplitude units, for $\sigma_1 = 0.15$, $\sigma_2 = \sigma_3 = 0.2$, $\sigma'_2 = \sigma'_3 = 0.4$, $\langle J \rangle = 1$, $A_1 = 1$, $A_2 = A_3 = 2$, and $A'_2 = A'_3 = 1$. We further assume for simplicity that $\langle A_i A_j \rangle = \langle A_i \rangle \langle A_j \rangle$ and $\langle A_1 A_2 A_3 \rangle = \langle A_1 \rangle \langle A_2 \rangle \langle A_3 \rangle$ although it is unlikely realized in practice. Panel (a) presents the cumulant for the Poissonian case, whereas panel (b) displays a non-Poissonian case for which $\langle J(J-1) \rangle - \langle J \rangle^2 / \langle J \rangle^2 = 0.05$. The peak centered at $\Delta\varphi_{12} = \Delta\varphi_{13} = 0$ corresponds to two particles associated with the high p_t particle, and is referred to as the near side jet peak. Secondary peaks at $(0, \pi)$, $(\pi, 0)$, and (π, π) correspond to one or both the associates being detected on the away side. The bands seen in Figure 1 (b) stem from the non-zero two-particle contributions to the 3-cumulant for non-Poissonian events. Various effects may alter the strength and shape of the jet correlations. Interactions of the parton with the medium may produce jet broadening, and deflection. Given jet emission is expected to be surface biased in $A + A$ collisions (in view of recent measurements of small R_{AA} , and the disappearance of the away side jet [48]), one expects the near side peak to have similar width in $A + A$ collisions as in $p + p$ collisions, while the away-side peak should be broader. One might also observe additional broadening along $\Delta\varphi_{12}$, and $\Delta\varphi_{13}$ due to parton scattering, and radial flow.

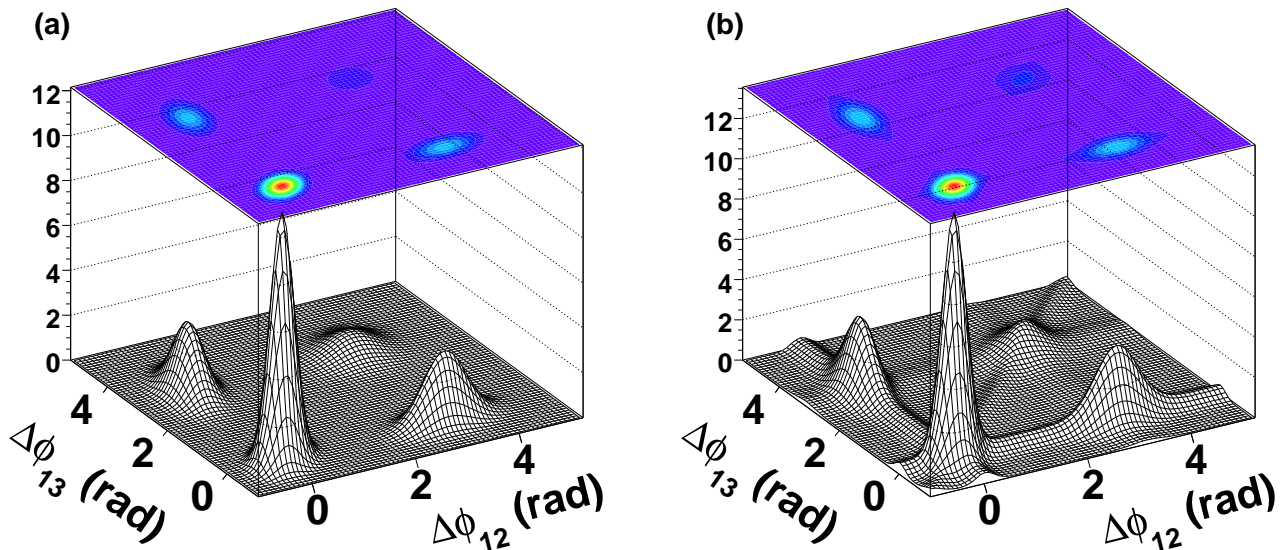


FIG. 1: 3-Cumulants calculated based on the Gaussian jet model discussed in the text. (a) Poisson case, (b) Non-Poisson case with $\langle J(J-1) \rangle - \langle J \rangle^2 = 0.05\langle J \rangle$

B. Collective Flow

Flow, or collective motion, is an important feature of heavy ion collisions at relativistic energies. It manifests itself by a modification of transverse momentum (p_t) spectra relative to those observed in $p + p$ collisions, and by azimuthal anisotropy of produced particles. In this section, we focus on azimuthal anisotropy arising in non-central heavy ion collisions. We decompose the azimuthal anisotropy in terms of harmonics relative to an assumed reaction plane. The conditional probability, $P_F(\varphi_i|\psi)$, to observe a particle at a given azimuthal angle, φ_i , with the reaction plane at

angle, ψ , is written as a Fourier series.

$$P_F(\varphi_i|\psi) = F_2(\varphi_i - \psi; v_m(i)). \quad (7)$$

where

$$F_2(\Delta\varphi; v_m) = 1 + 2 \sum_m v_m \cos(m(\Delta\varphi)) \quad (8)$$

The Fourier coefficients $v_m(i)$ measure the m -th order anisotropy for particles emitted in a selected kinematic range i . Measurements have shown the second order (elliptical) anisotropy can be rather large in $Au + Au$ collisions at RHIC while first and fourth order harmonics are typically much smaller. STAR measurements show the fourth harmonic scales roughly as the square of the second order harmonic ($v_4 \approx 1.1v_2^2$) [48, 49]. The third and fifth harmonics are by symmetry null at $\eta = 0$ for a colliding system such as $Au + Au$, and expected to be rather small at other rapidities. Higher harmonics are most likely negligible. We neglect possible event-to-event fluctuations of these coefficients given it emerges from recent works disentangling flow fluctuations and non-flow correlations is difficult. We describe the probability of finding N_i particles in the kinematical range i according to probability $P(N_i)$. The exact form of this probability is not required. Only its first, second, and third moments are needed. The joint probability of measuring N_i particles at an angle φ_i while the reaction plane angle is at ψ is given by $P_F(\varphi_i, N_i, \psi) = P_F(\varphi_i|\psi)P_F(N_i)P_{RP}(\psi)$ where $P_{RP}(\psi) = (2\pi)^{-1}$ is the probability of finding the reaction plane at a given angle ψ . Integration yields the single particle density $\rho_1(\varphi_i) = (2\pi)^{-1} \langle N_i \rangle$. The flow 2- and 3-cumulants are given respectively by (see Ref.[41] for a derivation of these expressions):

$$\begin{aligned} C_2^F(\Delta\varphi_{ij}) &= (2\pi)^{-2} (\langle N_i N_j \rangle F_2(\Delta\varphi_{ij}; v_m(i)v_m(j)) - \langle N_i \rangle \langle N_j \rangle) \\ &= (2\pi)^{-2} \langle N_i N_j \rangle \\ &\quad \times \left(1 - d_{ij} + 2 \sum_m v_m(i)v_m(j) \cos(m\Delta\varphi_{ij}) \right) \end{aligned} \quad (9)$$

and

$$\begin{aligned} C_3^F(\varphi_i, \varphi_j, \varphi_k) &= (2\pi)^{-3} \langle N_1 N_2 N_3 \rangle [\Phi_3(\varphi_i, \varphi_j, \varphi_k) \\ &\quad + (1 - f_{ijk}) \Phi_2(\Delta\varphi_{ij}) \\ &\quad + (1 - f_{ikj}) \Phi_2(\Delta\varphi_{ik}) \\ &\quad + (1 - f_{jki}) \Phi_2(\Delta\varphi_{jk}) \\ &\quad + 1 - f_{ijk} - f_{ikj} - f_{jki} + 2g_{ijk}] \end{aligned} \quad (10)$$

where

$$\Phi_2(x; v_{1,m}, v_{2,m}) = 2 \sum_{m=1}^{\infty} v_{1,m} v_{2,m} \cos(mx) \quad (11)$$

and

$$\Phi_3(\varphi_i, \varphi_j, \varphi_k) = 2 \sum_{p,m,n} v_{1,p} v_{2,m} v_{3,n} \begin{bmatrix} \delta_{p,m+n} \cos(p\varphi_i - m\varphi_j - n\varphi_k) \\ + \delta_{m,p+n} \cos(-p\varphi_i + m\varphi_j - n\varphi_k) \\ + \delta_{n,m+p} \cos(-p\varphi_i - m\varphi_j + n\varphi_k) \end{bmatrix} \quad (12)$$

$v_{i,m}$ correspond to the anisotropy coefficients of order m for particle i . The coefficients d_{ij} , f_{ijk} , and g_{ijk} are defined as follows

$$\begin{aligned} d_{ij} &= \frac{\langle N_i \rangle \langle N_j \rangle}{\langle N_i N_j \rangle} \\ f_{ijk} &= \frac{\langle N_i N_j \rangle \langle N_k \rangle}{\langle N_i N_j N_k \rangle} \\ g_{ijk} &= \frac{\langle N_i \rangle \langle N_j \rangle \langle N_k \rangle}{\langle N_i N_j N_k \rangle} \end{aligned} \quad (13)$$

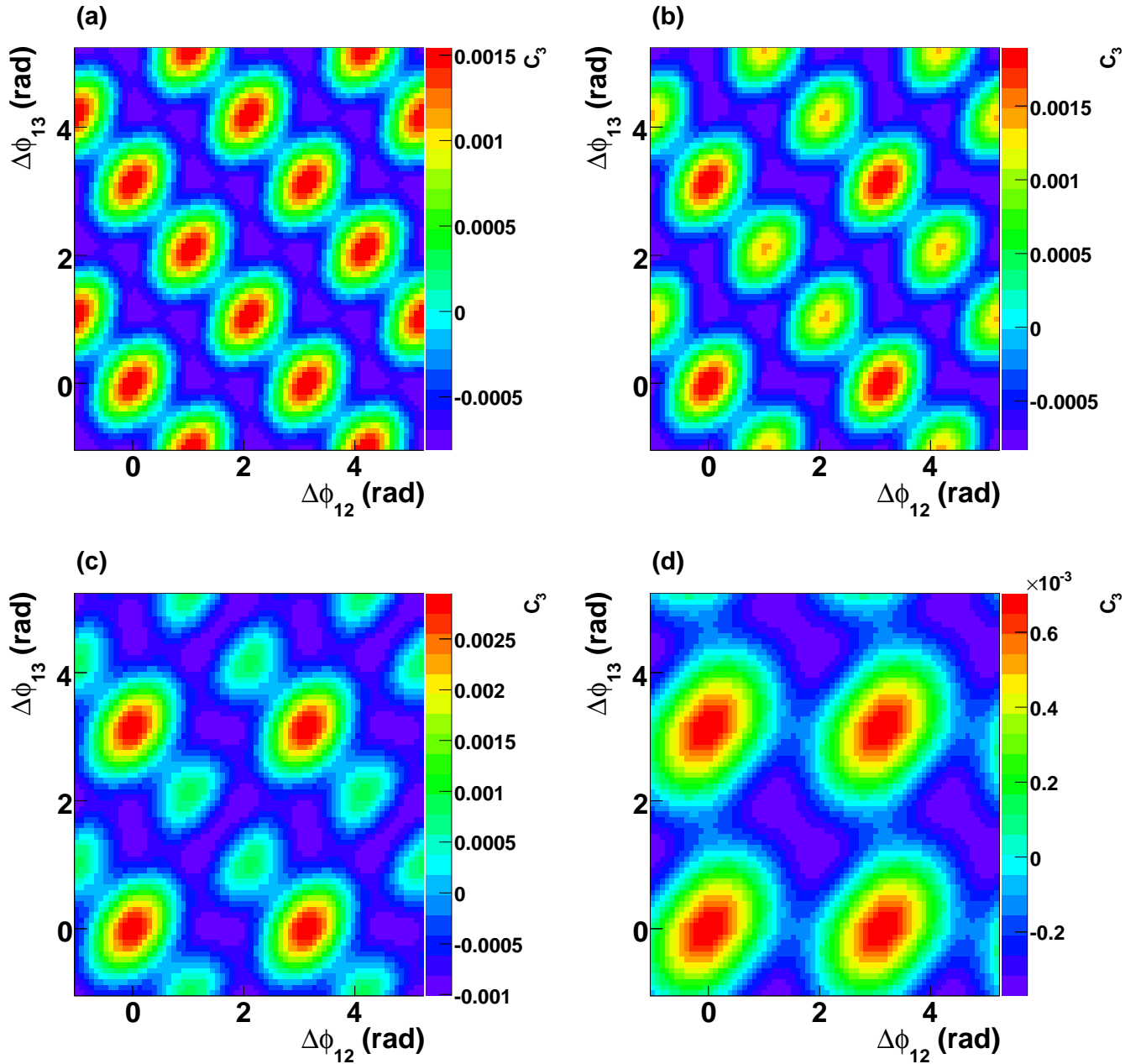


FIG. 2: 3-cumulant flow signal calculated using (a) only $v_2v_2v_4$ terms, (b) $v_2v_2v_4$ and $v_2v_2 + v_4v_4$ terms in 1:0.5 ratio, (c) $v_2v_2v_4$ and $v_2v_2 + v_4v_4$ terms in a 1:2 ratio, (d) only $v_2v_2 + v_4v_4$ terms. The $v_2v_2v_4$ and $v_2v_2 + v_4v_4$ terms are calculated according to Eqs. 11-14. See text for details.

We find that the flow 3-cumulant involves, in general, an arbitrary combination of second (e.g. v_2^2) and third order (e.g. $v_2v_2v_4$) terms. If particle production is strictly Poissonian, the coefficients f_{ijk} and g_{ijk} are unity. The second order terms of the cumulant thus vanish, and the 3-cumulant (flow only) then reduces to:

$$C_3^{F,Poisson}(\varphi_1, \varphi_2, \varphi_3) = (2\pi)^{-3} \langle N_1 N_2 N_3 \rangle \Phi_3(\varphi_1, \varphi_2, \varphi_3; v_p(1)v_m(2)v_n(3)) \quad (14)$$

which features only non-diagonal terms $v_m(i)v_n(j)v_p(k)$, i.e. with $m \neq n$, $m \neq p$, or $n \neq p$. This is illustrated in Figure 2 (a) which shows the flow 3-cumulant calculated using only $v_2v_2v_4$ terms. In general, particle production is non-Poissonian, and second order terms must be considered. The flow 3-cumulant shown in Fig. 2 (b) and (c) includes v_2^2 and v_4^2 added in ratios 1:0.5, and 1:2 respectively to the $v_2v_2v_4$ terms. Only v_2^2 and v_4^2 terms are included in Fig 2 (d) illustrating a case where non-Poisson fluctuations are very large, and thereby dominate the 3-cumulant. The

shape of the 3-cumulant thus depends significantly on the strength of the non-Poisson (2^{nd} order terms), as well as the magnitude of the flow coefficients. The interpretation of measured 3-cumulants may thus be considerably complicated by the presence of non-Poisson fluctuations.

Experimentally, one can estimate the magnitude of second order (diagonal) terms from measured total numbers of triplet, pair, and single particle densities. STAR observes based on data from Au + Au collisions at 200 GeV [46], the coefficients f_{123} and f_{231} deviate from unity. The size of the deviation scales qualitatively as the inverse of the event multiplicity. STAR also finds the magnitude of the deviation depends on the specific particle kinematic ranges used to carry the analysis. The particle production process is manifestly non-Poissonian. Since the bulk of produced particles exhibits elliptic flow, this implies the conditions $f_{ijk} = g_{ijk} = 1$ are not verified in practice. The second order and constant terms of the cumulant do not vanish, and may in fact be sizable. The 2^{nd} second order terms result from number fluctuations, and may in principle be estimated (and thus fitted) on the basis of measurements of f_{ijk} . Note however that multiplicity fluctuations occur for flow-like processes as well as all other types of production processes (including jets, conical emission, etc). It is thus non-trivial to unambiguously evaluate the proper magnitude of the diagonal flow terms based on ratios of measured yields.

Effects of flow fluctuations are not specifically addressed in the above flow model. Note however that, as defined, the 3-cumulant measures averages of $\langle v_n^2 \rangle$, and $\langle v_i v_j v_k \rangle$ coefficients rather than averages of $\langle v_n \rangle$. The 3-cumulant thus implicitly features fluctuations and non-flow effects. Given it is difficult to experimentally distinguish flow fluctuations and non-flow effects (see for instance the review by Voloshin *et al.* [50]), analyses attempting explicit subtraction of flow contributions (from three particle densities) based on the above equations, are thus intrinsically non-robust.

C. Conical Emission

Mach cone emission of particles by partons propagating through dense QGP matter was proposed by Stoecker [2] to explain the peculiar dip structure found at 180° in two-particle correlations reported by the STAR and PHENIX collaborations, and is the subject of many recent theoretical investigations [1, 2, 3, 4, 5, 6, 7, 8, 9, 10, 11, 22, 23, 24, 26, 27]. The concept of Mach cone emission is based on the notion that high momentum partons propagating through a dense QGP interact with the medium and lose energy (and momentum) at a finite rate. The release of energy engenders a wake that propagates at a characteristic angle, the Mach angle, determined by the sound velocity in the medium. Authors of Ref. [4] estimated the speed of sound in the QGP to be of the order of $v_s \approx c_s^{RHIC} \approx 0.33$. The Mach angle should thus be of the order of 70° relative to the away-side parton direction. We use this prediction to motivate a simple geometrical model of conical emission. The near-side jet is described using a Gaussian azimuthal profile. Away side particles are emitted at a cone angle of 1 radian with a scatter of 0.05 radian relative to the away-side direction. Figures 7 (a-b) present the 3-cumulant obtained with a Monte Carlo simulation based on two million events. Given that Mach cone particles are produced at 1 radian from the away-side direction and roughly normal to the beam direction, narrow Jacobian peaks are seen in the three-particle correlations. A strong dip is present at 180° in the two-particle correlations, while in the three-particle correlation a clear spacing is found between the peaks. In this simple model, the finite width of the peaks is due in part to the finite width of the trigger jet, and in part to the scatter imparted to the cone particles relative to the away-side direction. In practice, one might expect additional broadening of the cone because the speed of sound changes through the life of the QGP medium, and given the finite size of the medium. Radial flow might also significantly alter the correlation functions. As discussed in [41], the details of the correlation shapes clearly depend on assumptions made about the kinematics of the away-side parton.

D. Flow \times Jet Correlations

The measured nuclear modification factor, R_{AA} , defined as the ratio single particle yields measured in $A + A$ collision to those measured in $p + p$ interactions (scaled by the number of binary collisions in $A + A$) suggest the propagation of jets through the medium is severely quenched, and therefore features a surface emission bias [48]. In this scenario, partons propagating through the medium lose a large fraction of their energy. This results into jet lost or lower energy jets with smaller particle multiplicity. The path length through the medium determines the amount of energy loss and quenching. At a given point of emission, near the medium surface, a parton propagating outward in a direction normal to the surface should have shortest pathway through the medium, and minimal energy loss. Partons produced at the same location, but emitted in other directions would have longer path through the medium and suffer larger energy loss. In this scenario, one thus expects jet yields (and consequently the high p_t trigger) to be correlated to the reaction plane orientation. Neglecting disturbances imparted to the medium by the propagation

of the jet (or parton), we model the jet dependency on azimuthal angle relative to the reaction plane with Fourier decomposition. Specifically, we write the probability of the jet being emitted at angle ϕ while the reaction plane is at angle ψ as

$$P(\phi|\psi) = 1 + 2 \sum_n a_n \cos(n(\phi - \psi)) \quad (15)$$

where the coefficients a_n represent the effect of the differential azimuthal attenuation. We parameterize the jet multiplicity and azimuthal width using associated yields, and Gaussian widths that do not depend on the azimuthal direction. As in Sec. III A, the average number of jets per event is written $\langle J \rangle$ while the number of particles associated with a given jet is $\langle A_i \rangle$. We also assume the presence of a *flowing* background consisting on average of $\langle B_i \rangle$ particles. The single particle yield is thus $\rho_{1,J \otimes F}(\varphi_i) = (2\pi)^{-1} (\langle J \rangle \langle A_i \rangle + \langle B_i \rangle)$. Given the production of both jets, and background particles is correlated to the reaction plane, one ends up with flow-induced correlations between all particles, even those produced by the jets. The two-particle cumulant involves three sets of terms, namely jet-jet ($J \otimes J$), jet-background ($J \otimes B$), and background-background ($B \otimes B$). Similarly, the three-particle cumulant involves $J \otimes J \otimes J$, $J \otimes J \otimes B$, $J \otimes B \otimes B$, and $B \otimes B \otimes B$ terms.

A jet-flow model was already discussed in [41]. We here re-derive, and express the various terms of the model with a more compact and intuitive notation. The terms, $B \otimes B$ and $B \otimes B \otimes B$ are identical in form to those considered in Sect III B. We need to discuss only the terms $J \otimes J$, $J \otimes B$, $J \otimes J \otimes J$, $J \otimes J \otimes B$, and $J \otimes B \otimes B$. We begin with $J \otimes J$, and $J \otimes J \otimes J$. These terms contain contributions where two (three) of the particles are part of the same jet, and others where one, or two particles are not from the same jet. When particles are from the same jet, the correlation to the reaction plane is unimportant (to the extent, in our model, that the width of the jets do not change with their orientation relative to the reaction plane). The corresponding terms are thus identical to those obtained in the absence of flow. The two-particle density includes a term with two particles from the same jet (identical to that discussed in Sec. III A), and a term with particles from two different jets. This last term is given by:

$$\begin{aligned} \langle J(J-1) \rangle \langle A_i \rangle \langle A_j \rangle \int d\psi d\phi_\alpha G(\varphi_i - \phi_\alpha) \\ \times P(\phi_\alpha|\psi) \int d\phi_\beta G(\varphi_i - \phi_\beta) P(\phi_\beta|\psi) \end{aligned} \quad (16)$$

Integration, and inclusion of the first term yields the jet component of the two-particle density.

$$\begin{aligned} \rho_2^{Jetonly}(\varphi_i, \varphi_j) = \langle J \rangle \langle A_i A_j \rangle G_2(\varphi_i - \varphi_j; \sigma_{12}) \\ + \langle J(J-1) \rangle \langle A_i \rangle \langle A_j \rangle F_2(\varphi_i - \varphi_j; a_n(i, j)) \end{aligned} \quad (17)$$

where $\sigma_{12}^2 = \sigma_1^2 + \sigma_2^2$, $a_n(i, j) = v'_n(i)v'_n(j)$, with $v'_n(i) = a_n \exp(-n^2\sigma_i^2/2)$. Similarly, the three-particle density includes a term with three particle from the same jet, two particles from the same jet, and another with all three particles from different jets. The $J \otimes J$, and $J \otimes J \otimes J$ part of the cumulant is as follows.

$$\begin{aligned} \rho_3^{Jetonly}(\varphi_i, \varphi_j, \varphi_k) = \langle J \rangle \langle A_i A_j A_k \rangle G_3(\varphi_i, \varphi_j, \varphi_k; \sigma_i, \sigma_j, \sigma_k) \\ + \langle J(J-1) \rangle \langle A_i A_j \rangle \langle A_k \rangle G_2(\Delta\varphi_{ij}) F_2 \left(\frac{\sigma_j^2}{\sigma_{ij}^2} \varphi_i + \frac{\sigma_i^2}{\sigma_{ij}^2} \varphi_j - \varphi_k; v''_n(k) \right) + (jki) \\ + \langle J(J-1)(J-2) \rangle \langle A_i \rangle \langle A_j \rangle \langle A_k \rangle N_3(\varphi_i, \varphi_j, \varphi_k; v'_n(i), v'_m(j), v'_p(k)) \end{aligned} \quad (18)$$

The functions G_3 , F_3 , F_2 were defined in previous sections. The symbol (jki) indicates identical terms obtained by permutation of the indices. The term G_3 is identical to that obtained for non-flowing jets. The term of the last row corresponds to a flow-like correlation between the three measured particles, albeit with a strength which depends on the fluctuations of the number of jets per event, and the jet associated multiplicities in the kinematic ranges considered. The second row contains three similar terms that embody the jet-flow correlations: two particles are correlated because they belong to the same jet, while the third is correlated to the first two because of reaction plane dependencies. One notes that in the above expression, F_2 depends on the angle of emission of all three particles (at variance with assumptions made in Ref. [31, 32]) in a non trivial way. Indeed, in general, the jet correlation widths σ_i depend on the particle momentum ranges: the ratios σ_i^2/σ_{ij}^2 are arbitrary (non-integer) values. F_2 therefore involves inharmonic flow components. This implies it is inappropriate to model jet-flow cross-terms as a simple product of jet-like correlations, and flow-like correlations, as in Ref. [31, 32], for purposes of background subtraction.

We next consider the component $J \otimes J \otimes B$, and $J \otimes B \otimes B$ of the 3-cumulant. Following the steps used for the derivation of the pure jet components, one finds it also includes a term proportional to $F_2 G_2$ indistinguishable from

$J \otimes J \otimes J$. One has

$$\langle J \rangle \langle A_1 A_2 \rangle \langle B_3 \rangle G_2(\Delta\varphi_{12}; \sigma_{12}) F \left(\frac{\sigma_2^2}{\sigma_{12}^2} \varphi_1 + \frac{\sigma_1^2}{\sigma_{12}^2} \varphi_2 - \varphi_3; v_n''(3) \right) \quad (19)$$

The $J \otimes B \otimes B$ component of the 3-cumulant contains a non-diagonal flow term as follows

$$\langle J \rangle \langle A_1 \rangle \langle B_2 B_3 \rangle F_3(\varphi_i, \varphi_j, \varphi_k; v_n'(i), v_m'(j), v_p'(k)) \quad (20)$$

This term has the same functional dependence and is indistinguishable from the term on the third line of Eq 19. Assembling all components, one obtains the JET \otimes FLOW 3-cumulant:

$$\begin{aligned} C_3^{J \otimes F}(\varphi_i, \varphi_j, \varphi_k) &= \langle J \rangle \langle A_i A_j A_k \rangle G_3(\varphi_i, \varphi_j, \varphi_k; \sigma_i, \sigma_j, \sigma_k) \\ &+ \left(\langle J(J-1) \rangle - \langle J \rangle^2 \right) \langle A_i A_j \rangle \langle A_k \rangle G_2(\Delta\varphi_{ij}) + (jki) \\ &+ \langle A_i A_j \rangle (\langle J(J-1) \rangle \langle A_k \rangle + \langle J \rangle \langle B_k \rangle) G(\Delta\varphi_{ij}; \sigma_{ij}) \Phi_2 \left(\frac{\sigma_j^2}{\sigma_{ij}^2} \varphi_i - \frac{\sigma_i^2}{\sigma_{ij}^2} \varphi_j - \varphi_k; v_n''(k) \right) + (jki) \\ &- \langle J(J-1) \rangle \langle A_i \rangle \langle A_j \rangle \langle A_k \rangle F_2(\varphi_i - \varphi_j; a_n(i, j)) + (jki) \\ &+ \langle J(J-1)(J-2) \rangle \langle A_i \rangle \langle A_j \rangle \langle A_k \rangle N_3(\varphi_i, \varphi_j, \varphi_k; v_n'(i), v_m'(j), v_p'(k)) \\ &+ \langle J \rangle \langle A_i \rangle \langle B_j B_k \rangle N_3(\varphi_i, \varphi_j, \varphi_k; v_n'(i), v_m'(j), v_p'(k)) \\ &- \langle B_i B_j \rangle \langle J \rangle \langle A_k \rangle F_2(\varphi_i - \varphi_j; v_n(i)v_n(j)) + (jki) \\ &+ (2\pi)^{-3} \langle B_i B_j B_k \rangle \Phi_3(\varphi_i, \varphi_j, \varphi_k; v_p(i)v_m(j)v_n(k)) \\ &+ (2\pi)^{-3} \langle B_i B_j B_k \rangle (1 - f_{ijk}) \Phi_2(\varphi_i - \varphi_j; v_m(i), v_m(j)) + (jki) \\ &- (2\pi)^{-3} \langle B_i B_j B_k \rangle f_{ijk} + (jki) \\ &+ \text{constants} \end{aligned} \quad (22)$$

This cumulant includes components typical of jets (line 1 and 2), flow (line 4-11'), and one term unique to jet-flow cross-term (line 3). While this jet-flow term does include two-particle jet-like, and flow-like factors, it is important to note the flow factor is intrinsically inharmonic. Its amplitude depends on the number jet associates and background particle multiplicity. Given the number of associates is likely much smaller than the number of background particles, one expects the amplitude of this term to be dominated by the magnitude of the background. It is interesting to compare the magnitude of this cross-term relative to the off-diagonal flow terms. We focus on the difference between the leading terms in $v_2 v_2 v_4$ and $v_2 v_2$. Given the jet cross section and fragment multiplicity are small at RHIC energies, one expects the $v_2 v_2 v_4$ term should dominate or at most be of similar magnitude to the cross-term unless the jet flow v_2 is considerably larger than the bulk flow.

As discussed in Sect III B, particle emission in $A + A$ collisions is a non-Poissonian process. The coefficients f_{ijk} in general deviate from unity. The leading background terms may thus be those of line 2, 6, 7, and 9 in Eq. 22.

Lines 4 and 7 both contain terms in F_2 albeit with different amplitudes. Experimentally these cannot be distinguished, and one ends up with an F_2 contribution to the cumulant which depends on both the jet and background yields. Likewise, lines 5, 6, 8, and 9 feature non-diagonal flow terms (dominated by $v_2 v_2 v_4$) which cannot be distinguished experimentally: the amplitude of the $v_2 v_2 v_4$ three particle correlation terms depend intricately on the jet yield, its fluctuations, as well as the background yield. The jet-flow 'cross-term' manifests itself through the inharmonic terms of line 3 in Eq. 22. While these harmonic terms may be approximated as a product such as $G_2(\Delta\phi_{12}) F \Phi_2(\Delta\phi_{13})$ if the width σ_1 (very high- p_t particles) is negligible, when added in quadrature, to the width σ_2 of the low- p_t particle, the approximation breaks down in general because σ_1 is neither zero or equal to σ_2 . Additionally, note that the model used in this section assumed the cross-terms are dominated by jetty and flow components. This may not be the case in practice. For instance resonance or cluster decays in the presence of both radial and elliptical flow should lead to complex cross terms. Such cross-terms shall be inherently inharmonic also. Given the correlation shapes associated with resonance or cluster decays can be quite wide, the inharmonic character of the cross term can be quite intricate. Adhoc subtraction of terms in $G_2(\Delta\phi_{12}) F \Phi_2(\Delta\phi_{13})$ in model based analyses is therefore unwarranted.

IV. PROBABILITY CUMULANTS

We showed in Section III B that the 3-cumulant associated with flow reduces to non-diagonal terms in $v_n v_m v_p$ for Poissonian particle production processes. However, momentum, energy, and quantum number conservation laws

imply elementary collisions are typically non-Poissonian processes as observed from Fig 3 which shows ratios f_{ijk} measured by STAR [46]. This implies the 3-cumulant may have a rather complicated structure, with second order terms (i.e. two-particles) as well as three particle terms. We note however that the simplicity of the 3-cumulant may be recovered, in this case, by using probability cumulants rather than density cumulants. The probability cumulants are defined as follows:

$$\begin{aligned}
P_2(\varphi_i, \varphi_j) &\equiv \frac{\rho_2(\varphi_i, \varphi_j)}{\langle N_i N_j \rangle} - \frac{\rho_1(\varphi_i)\rho_1(\varphi_j)}{\langle N_i \rangle \langle N_j \rangle} \\
P_3(\varphi_i, \varphi_j, \varphi_k) &\equiv \frac{\rho_3(\varphi_i, \varphi_j, \varphi_k)}{\langle N_i N_j N_k \rangle} - \frac{\rho_2(\varphi_i, \varphi_j)\rho_1(\varphi_k)}{\langle N_i N_j \rangle \langle N_k \rangle} \\
&\quad - \frac{\rho_2(\varphi_i, \varphi_k)\rho_1(\varphi_j)}{\langle N_i N_k \rangle \langle N_j \rangle} - \frac{\rho_2(\varphi_j, \varphi_k)\rho_1(\varphi_i)}{\langle N_j N_k \rangle \langle N_i \rangle} \\
&\quad + 2 \frac{\rho_1(\varphi_i)\rho_1(\varphi_j)\rho_1(\varphi_k)}{\langle N_i \rangle \langle N_j \rangle \langle N_k \rangle}
\end{aligned} \tag{23}$$

where N_i correspond to total particle multiplicities accepted in the kinematic cuts i . It is straightforward to verify that the flow probability 3-cumulant indeed consists of non-diagonal flow terms only:

$$P_3^N(\varphi_1, \varphi_2, \varphi_3) = (2\pi)^{-3} \Phi_3(\varphi_1, \varphi_2, \varphi_3; v_p(1)v_m(2)v_n(3)) \tag{25}$$

The probability cumulant, P_3 , thus provides a tool to suppress the strength of non-Poissonian 2^{nd} order terms, and may therefore be used, in addition to the number 3-cumulant, C_3 , in three-particle analyses.

The simplification obtained for flow processes is unfortunately not realized for jet or conical emission processes. The use of probability 3-cumulant may then be of limited interest in practice. This can be straightforwardly shown through a calculation of the probability cumulant of the Gaussian model used in Sec. III A. We limit our calculation to the near side jet. One finds the probability 3-cumulant contains terms in $G_2(\Delta\phi)$ proportional to the non vanishing factor $\langle J(J-1) \rangle \langle N_1 N_2 \rangle \langle N_3 \rangle - \langle J \rangle^2 \langle N_1 N_2 N_3 \rangle$, where N_1 , $N_1 N_2$, and $N_1 N_2 N_3$ are respectively the number of singles, pairs, and triplets from the near side jet. By contrast to the flow probability 3-cumulant which contains only genuine three-particle correlation terms (Φ_3), the Gaussian probability cumulant thus has a complicated expression which contains terms in G_3 as well as in G_2 . Its interpretation is therefore non trivial.

V. EFFICIENCY CORRECTION AND OBSERVABLE ROBUSTNESS

Measured particle densities, and cumulants must be corrected for detection efficiencies and other instrumental effects. We introduced in Ref. [41] a procedure to correct for detector efficiencies based on ratios of two- and three-particle densities by products of two, and three single particle densities. For instance, up to a global efficiency factor, the corrected three-particle density is given by

$$\rho_3(\varphi_1, \varphi_2, \varphi_3)_{corrected} = (2\pi)^{-3} N(1)N(2)N(3) \frac{N_3(\varphi_1, \varphi_2, \varphi_3)}{N_1(\varphi_1)N_1(\varphi_2)N_1(\varphi_3)} \tag{26}$$

where $N_1(\varphi_i)$ stands for uncorrected single particle densities, $N_3(\varphi_1, \varphi_2, \varphi_3)$ are numbers of triplets, and $N(i)$ are total particle yields within the kinematics cuts i .

This correction procedure is strictly exact for continuous functions provided the efficiency is a function of the azimuthal angles φ_i but independent of other observables such as the particle rapidity and transverse momentum. For large detectors such as the STAR TPC [45], the efficiency is a smooth and slowly varying function of the pseudorapidity and transverse momentum, but exhibit periodic structures in azimuth because of TPC sector boundaries. A correction for azimuthal dependencies of the detector response is thus the most important and relevant in this context.

We examine the robustness of the above correction procedure in a practical situation, i.e. where the densities are measured with a finite number of bins, based on the jet and conical emission models discussed in Sec. 2. We parameterize the detection efficiency, $\varepsilon(\varphi_i)$, with a Fourier decomposition.

$$\varepsilon(\varphi_i) = \varepsilon_0 \left(1 + 2 \sum_{n=1}^{\infty} \varepsilon_n \cos(n\varphi_i) \right) \tag{27}$$

where ε_0 is the average efficiency, and coefficients ε_n determine the azimuthal dependence of the efficiency. We assume the efficiency for simultaneously detecting two and three particles are factorizable as product of single particle

efficiencies. The mean single particle detection efficiency is set to 80%. The Fourier coefficients (Eq. 27) are chosen to obtain a non-uniform azimuthal detector response as shown in Fig. 3. The JET+Mach Cone model described in

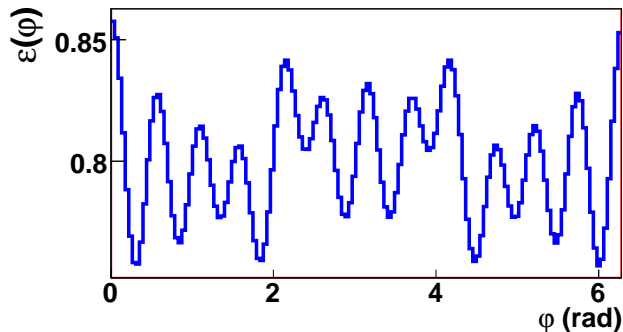


FIG. 3: (Color online) Detection efficiency dependence on the particle azimuthal angle used in the simulation results presented in Fig. 4.

sections III C and VI is used to carry a simulation of the robustness of the correction procedure. Figure 4 (a) displays the 3-cumulants obtain with perfect detection efficiency. Figure 4 (b) shows the uncorrected two particle density $\rho_2(\varphi_1, \varphi_2)$ obtained with the non-uniform azimuthal response illustrated in Fig 3. The two particle density exhibits strong, narrow, and repeated structures that result from the twelve-fold structure of the assumed detector response. Figure 4 (c) displays the 3-cumulant obtained with the same detector response, but corrected for efficiency effects by division of the two and three particle densities by the product of single particle densities, as in Eq. 26. In stark contrast to the correlation shown in Figure 4 (b), one finds the corrected cumulant exhibits no evidence of the detector response except for a global change in amplitude corresponding to the cube of the average detection efficiency. Figure 4 (d) shows the difference between this cumulant and the perfect efficiency cumulant scaled down by the cube of the average detection efficiency. The standard deviation of the difference is smaller than 1% of the maximum 3-cumulant amplitude and exhibit no particular structure. We thus conclude the correction method is numerically robust for cases where the triplet, and pair efficiencies factorize.

VI. CUMULANT METHOD SENSITIVITY FOR JET AND CONICAL EMISSION MEASUREMENTS

We present in this section a study of the sensitivity of the cumulant method described in this paper for a search for conical emission. Our study of the sensitivity of the method is based on Monte Carlo (MC) simulations carried out using a simple event generator that encapsulates flow, jet, and conical emission as a multicomponent model.

We begin our presentation of the simulations with flow-only model components. The overall multiplicity, noted m , of an event is selected randomly according to a flat distribution. The flow component is designed to produce, on average, a fraction, f_i , of the event multiplicity. The number of *flowing* particles, N_i , (for a kinematic cut i) is generated event-by-event randomly with a Poisson probability density function (PDF) of mean $m \times f_i$. The particle direction, in azimuth, is selected randomly according to the flow PDF given by Eq. 7. Various values of the coefficients v_2 and v_4 , which determine the magnitude of the bulk flow, are used in the following to study the impact of flow on the cumulant and sensitivity to a cone signal. All other Fourier coefficients are set to zero. The event plane azimuthal angle is chosen randomly in the range $[0, 2\pi[$. The coefficient f_1 is set to produce a number of high- p_t particles or order unity in each event, while f_2 is set to produce a low p_t particle multiplicity of order 100. These values are selected to mimic STAR data in the range $3 < p_t < 20$, and $1 < p_t < 2$ for the trigger and associate particles respectively.

Figure 5 (a) and (b) respectively display the triplet density and the 3-cumulant obtained with the above flow random generator with $v_2 = 0.1$, and $v_4 = 0$. The 3-cumulant, shown in Fig 5 (b), exhibits a finite v_2^2 component owing to the fact that although the multiplicities N_i are generated with Poisson PDFs, the mean of these PDFs varies as a function of the event multiplicity thereby implying a correlation between the low and high p_t particle multiplicities. This, in turn, implies the coefficients f_{ijk} are non-zero: the cumulant therefore contains a non-vanishing v_2^2 component. This component however vanishes in the probability cumulant shown in Fig 5 (c) as expected from Eq. 25.

Figure 6 shows results of a simulation based on the same flow model as that used in Fig. 5, but with an added fourth harmonic component. Flow amplitudes are set to $v_2 = 0.1$ and $v_4 = 0.01$. While the 3-particle density (Fig 6 (a)) is completely dominated by the 2^{nd} harmonic, one finds the 3-cumulant suppresses this component significantly (Fig 6 (b)), and enables clear observation of the $v_2^2 v_4$ non-diagonal terms expected from Eq. 24. The v_2^2 component

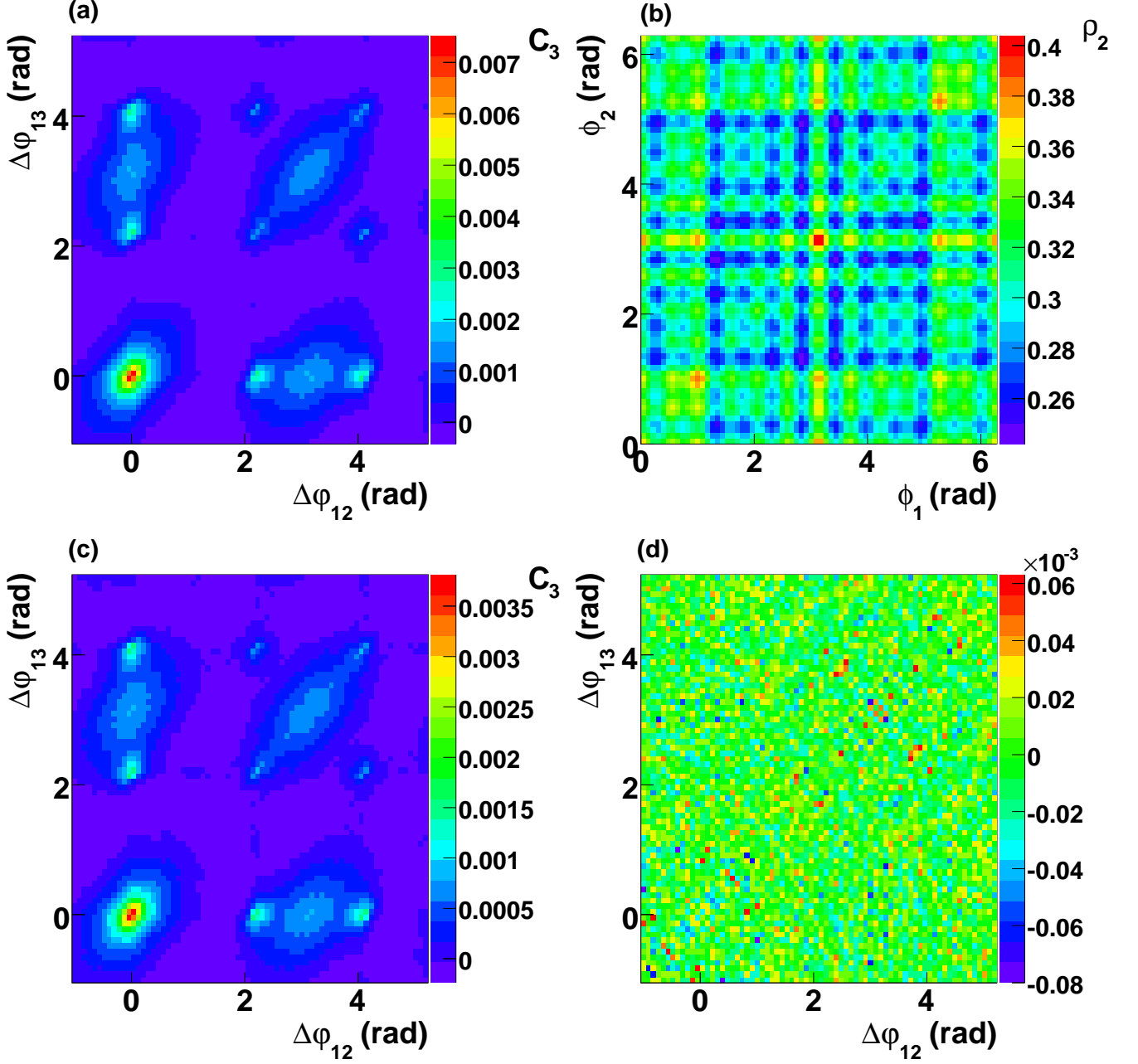


FIG. 4: Study of the efficiency correction method (Eq. 26) using the Mach Cone model described in Sec. VI. (a) 3-cumulant for perfect detection efficiency, (b) Two particle density, (c) 3-cumulant obtained with the azimuthal efficiency dependence shown in Fig. 3, (d) Difference between the 3-cumulants shown in (b), and the perfect efficiency cumulant scaled by the cube of the average detection efficiency.

is further suppressed in the probability cumulant, shown in Fig 6 (c), where only the $v_2^2 v_4$ component manifestly remains. As anticipated based on Eq. 25, the probability cumulant enables essentially full suppression of v_2^2 terms, and show irreducible flow components only.

Mono-jets and conical emission are next added to the simulated events. The jet axis (corresponding to the parton direction initiating the jet) is chosen randomly in the transverse plane. Particles are generated at random polar angles, relative to the jet direction using Gaussian PDFs. The width of the Gaussian is set to 0.15 radian for high p_t particles, and 0.25 for low p_t particles. Note that the conclusions of this study are essentially independent of the width of the jets. The associate multiplicity are generated jet-by-jet using Poisson PDFs. The near side jet associated particle multiplicity (i.e. number of associates per jet) are set to 1 and 2 for the high- and low- p_t particles respectively. No

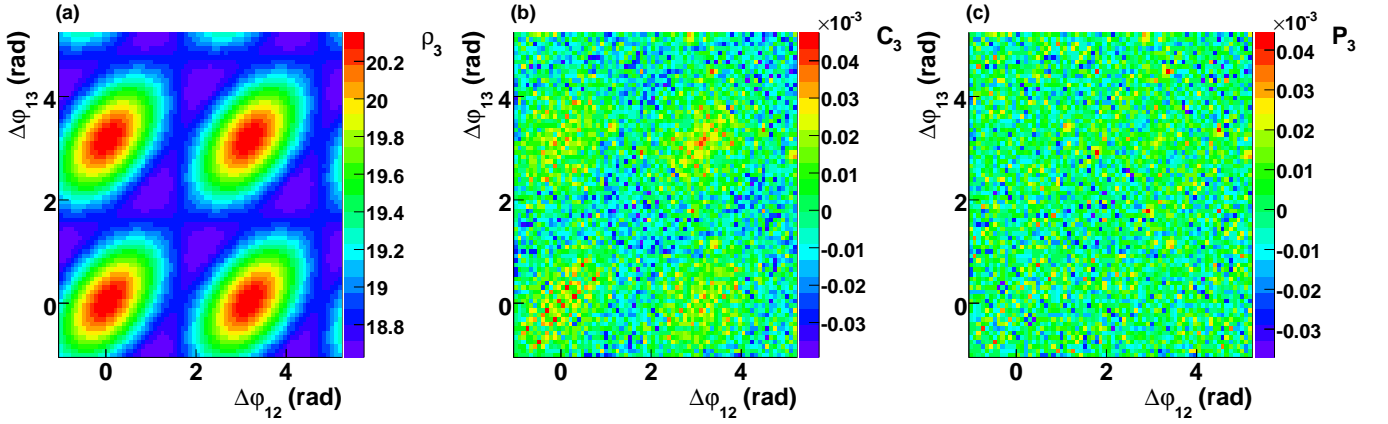


FIG. 5: Simulations of (a) the three-particle density, (b) three-cumulant, and (c) the probability cumulant for particle emission with elliptic anisotropy $v_2 = 0.10$.

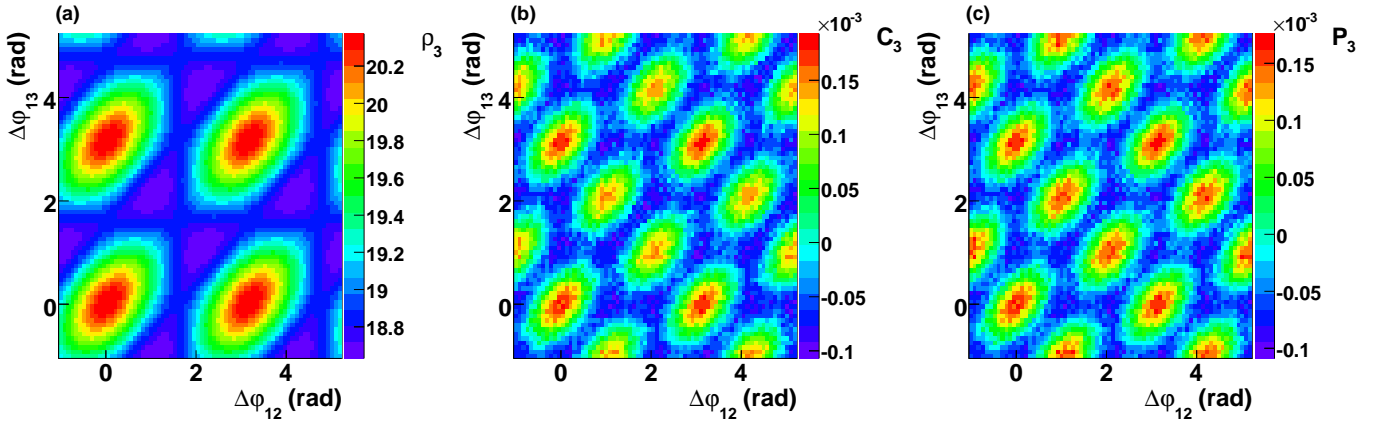


FIG. 6: Simulations of (a) the three-particle density, (b) three-cumulant, and (c) the probability cumulant for particle emission with elliptic anisotropy $v_2 = 0.10$, and $v_4 = 0.01$.

away side jet is included. Instead, one introduces a conical emission as described in the following. Jet parameters are selected to correspond approximately to associate jet yields measured by the CDF collaboration for jets of 10 to 20 GeV [47], as well as jet associated yields reported by RHIC experiments [52]. The number of jets is generated event-by-event with a Poisson PDF of mean 0.01 jet per unit multiplicity: the average number of jets per event is thence of order 1-2. Such large values are used to ease our study. Smaller, perhaps more realistic jet-yield values result in a weaker signal. This limits the statistical significance of the measurement, but does not constitute an intrinsic limitation of the cumulant method.

In our simulations, the parton determining the direction of the jet is first generated, and is restricted for simplicity to the reaction transverse plane. The away-side parton is emitted in the transverse plane as well, at angle of π radian relative to the jet parton. Conical emission is simulated by generating particles at a random polar angle relative to the away-side parton direction. The azimuthal direction of the particle, in the plane transverse to the parton direction, is randomly selected based on a uniform distribution. The polar angle is chosen to have a Gaussian distribution with an average value of one (1) radian. The number of high- p_t particles produced in this cone is arbitrarily set to zero, while the number of low- p_t cone particles in a given parton-parton collision is selected randomly with a Poisson distribution of mean equal two, unless specified otherwise in the following.

Because the cone particles are emitted at an arbitrary polar angle, but detected in the transverse plane as a function of relative azimuthal angles only, conical emission results in four Jacobian peaks, as seen in Fig. 7 (a). In order to characterize the shape and strength of these peaks, we use projections of the cumulants along the diagonals $\varphi_{12} + \varphi_{13} - 2\pi$ and $\varphi_{12} - \varphi_{13}$. Projections, shown in Fig. 7 (b) are limited to include narrow angular ranges about the diagonals. Specifically, the range $|\varphi_{12} - \varphi_{13}| < 10^\circ$ is integrated to obtain the projection along the plot main diagonal (displayed in red), whereas the condition $|(\varphi_{12} + \varphi_{13}) - 2\pi| < 10^\circ$ is used for projections along $\varphi_{12} - \varphi_{13}$ (shown in blue).

At issue is whether or not one can extract a cone signal given the presence of background particles, and flow. We thus vary the strength of the jet signal to background ratio by changing the fractional jet and background yields. Figures 7 through 11 show cumulants and projections obtained with various model parameters. All plotted cumulants were obtained with simulations integrating two millions events.

Figures 7 (a-b) shows the cumulant and projections obtained for an average of 2.5 jets per event. The number of high and low p_t particles associated with the jet, and cone are set respectively to 1 and 2. The uncorrelated background of high- and low- p_t particle are set to 2.5 and 100 particles per event respectively. The cone signal obtained with such parameters is obviously strong and clearly observable. Figure 7 (c) displays the cumulant and projections with a high- p_t background raised by a factor of 4 resulting in a signal to noise ratio of 25%. The observed cone strength remains unchanged, as expected given the background is uncorrelated. We also verified that an increase of the width of the gaussian PDF used for jet, and cone particle emission results in wider peak structures with reduced amplitude but no actual change in the integrated cone signal strenght. In this context, we conclude the observability of conical emission is only limited by the statistical accuracy of the measurement relative to the actual strength of the signal. For instance, a reduction by a factor of five of the number of high- p_t associated particles results in cone-signal five times small in amplitude, but the shape of the cumulant remains unchanged and the observability of the signal is thus only limited by the size of the event sample, and the number of particles associated with the trigger and cone.

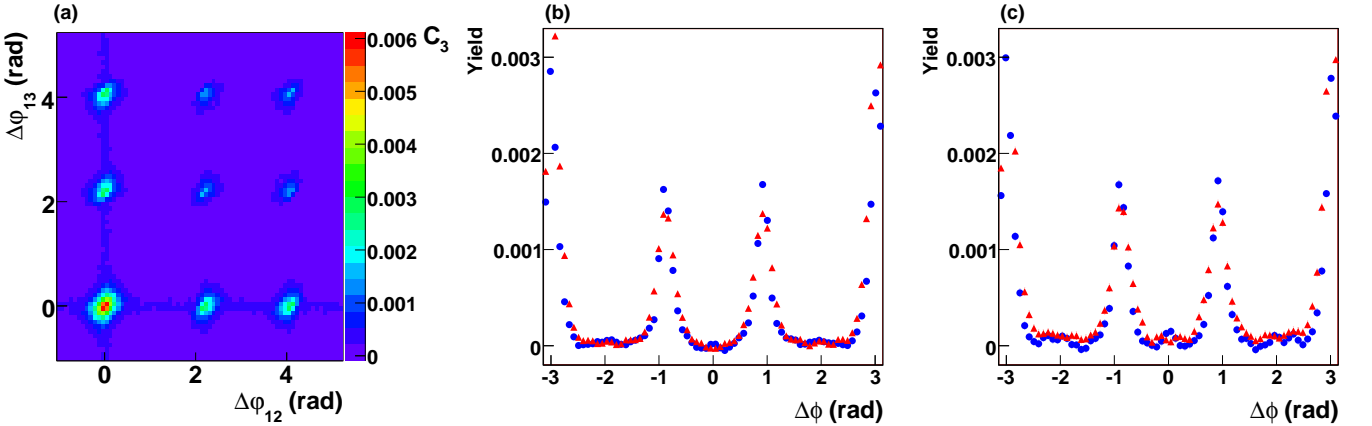


FIG. 7: (a) Simulation of the 3-cumulant obtained with mono-jet, conical emission, and background particles (without flow). Average jet yield to high- p_t particle background yield set to 1. (b) Projections of the cumulant along the main (red) and alternate (blue) diagonals for jet/cone parameters used in (a). Other particle generation parameters, and projections are discussed in the text. (c) Cumulant projections obtained for a high- p_t background to jet-signal ratio of 4.

We next consider the observability of conical emission in the presence of anisotropic flow. Figure 8 shows the cumulant and projections in the presence of a flow background. The jet and conical signals are identical to those used in Fig. 7 (a-b). An average background of 100 low- p_t particles is included with $v_2 = 0.1$, and $v_4 = v_2^2$. No high- p_t background is included. The cone signal shape and strength remains unaffected, although the projections exhibit a background structure somewhat more complex than that observed in Fig. 7. Fig. 8 (c) displays the projections obtained when the elliptic flow is raised to $v_2 = 0.2$. While the signal is clearly visible, one observes the emergences of cosine structures along the $\Delta\phi_{23}$ projection. These stem from the non-Poisson nature of the background multiplicity fluctuations used in the simulations.

Flow-like or cosine structures also appear when high- p_t background particles are added as shown in Figure 9 where the average high- p_t particle background is set to 2.5/event. The observability of the cone depends on its amplitude relative to that of the background, as well as on the magnitude of v_2 and v_4 . We note that the signal remains visible in the $\Delta\phi_{23}$ projection, with the jet and cone parameters used in Figure 7, even when the high- p_t background is raised by a factor of eight as shown in Fig. 9. For substantially larger background, the signal however becomes more difficult to extract as illustrated in Figure 10 where a background to signal ratio of sixteen is used for high- p_t particles. Clearly, the observability of a cone signal in the presence of flow depends on the strength of the signal relative to that of non-Poisson components and values of v_2 .

The model independent extraction of a conical signal becomes increasingly difficult as the signal strength is reduced and the elliptic flow magnitude increased. The measurement becomes particularly challenging when the jet amplitude is modulated by differential attenuation relative to the reaction plane, i.e. in the presence of jet-flow. Figures 11 (a) and (b) display projections along $\Delta\phi_{12} + \Delta\phi_{13}$ and $\Delta\phi_{23}$ obtained with jet $v_2 = 0.05$, (as defined in Sec. IIID). The blue squares and red circles show, respectively, the signals obtained with an average of two and one low- p_t particles involved in conical emission. Simulations are carried out with an average number of 2.5 jets/cones per event.

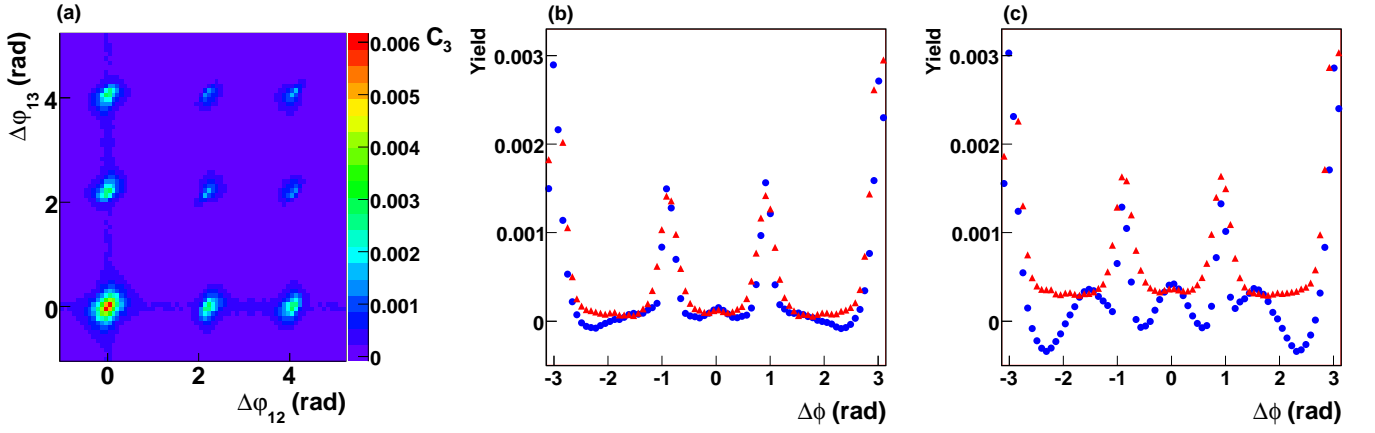


FIG. 8: Idem Fig. 7 in the presence of background flow. (a-b) No background high- p_t particle. Average of 100 low- p_t background particle per event, with flow $v_2 = 0.1$, and $v_4 = v_2^2$. (c) Average of 100 low- p_t background particle per event, with flow $v_2 = 0.2$, and $v_4 = v_2^2$.

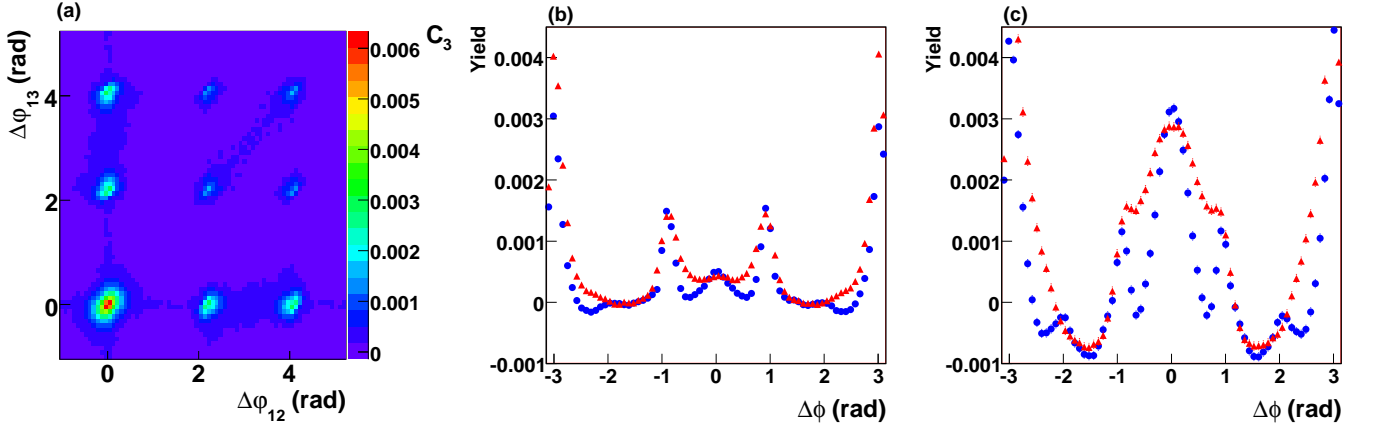


FIG. 9: (a-b) Idem Fig. 7 for average jet yield to high- p_t background equal one per event. Average of 100 low- p_t background particle per event, with flow $v_2 = 0.1$, and $v_4 = v_2^2$. (c) Projections obtained for average jet yield to high- p_t background equal eight (8) per event.

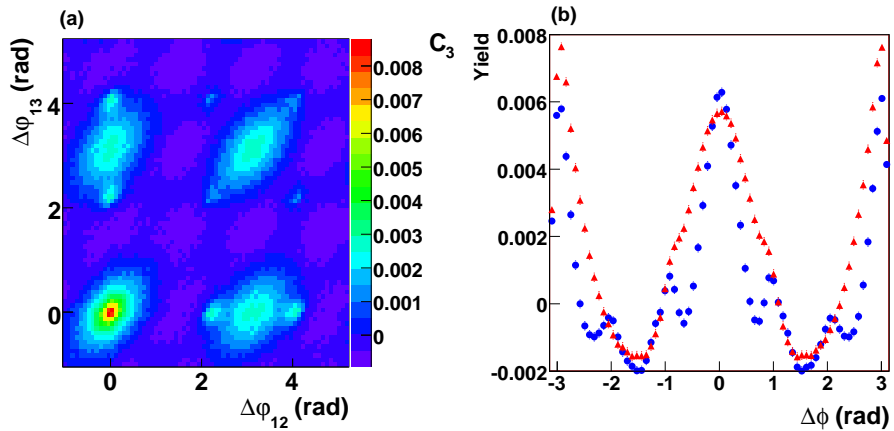


FIG. 10: Idem Fig. 7 for average high- p_t background to jet yield equal sixteen (16). Average of 100 low- p_t background particle per event, with flow $v_2 = 0.1$, and $v_4 = v_2^2$.

The average yield of high- p_t low- p_t background particle are set to 8 and 100 per event respectively. Background particles are produced with flow $v_2 = 0.1$, and $v_4 = v_2^2$. In our simulation, the number of cone associated particles is

determined event-by-event with a Poisson random number generator. The conical signal is detectable, in the context of this 3-cumulant analysis, only when two, or more, particles are generated per event. For an average cone yield of two associated particles, 60% of the cone events contain two or more cone particles. By contrast, only 26% of the events contain two cone particles when the average (cone) yield is one. The signal obtained in the former case is clearly visible, while it becomes weaker in the latter. The detectability of the signal thus greatly depends of the actual yield of conical emission. We note that two-particle correlation analyses report an away side yield of two particle per trigger after flow background subtraction based on a ZYAM hypothesis [51]. If this away side is due to conical emission, this implies the low- p_t cone particle average multiplicity is large and should therefore be detectable in the context of a 3-cumulant analysis. We note however that the cumulant measurements reported by the STAR collaboration at recent conferences do not exhibit as strong $\cos(2\Delta\varphi)$ components as those illustrated in the $\Delta\varphi_1 + \Delta\varphi_2$ projections shown in Fig. 11 [42]. Note additionally that the cone signal remains visible in the $\Delta\varphi_{23}$ projection even for small signal to background ratios. It is however obvious that strong background flow and jet-flow may hinder the observation of conical emission. For instance, Figure 12 shows a comparison of the 3-cumulant projections obtained for conical emission in the presence of jet-flow cross terms with v_2 values of 0.05 (blue) and 0.1 (red) an associate cone yield of one. One finds the cone signal is difficult to distinguish for $v_2 = 0.1$ but straightforward to observe for $v_2 = 0.05$.

In summary, we find in the context of our multicomponent model that the exact sensitivity of the measurement is a "complicated" function of the flow and background parameters of the model, and cannot readily be expressed in analytical form or even as a table. We further note that the shape and strength of actual correlations is influenced by momentum, and quantum number conservation effects not explicitly addressed in this work.

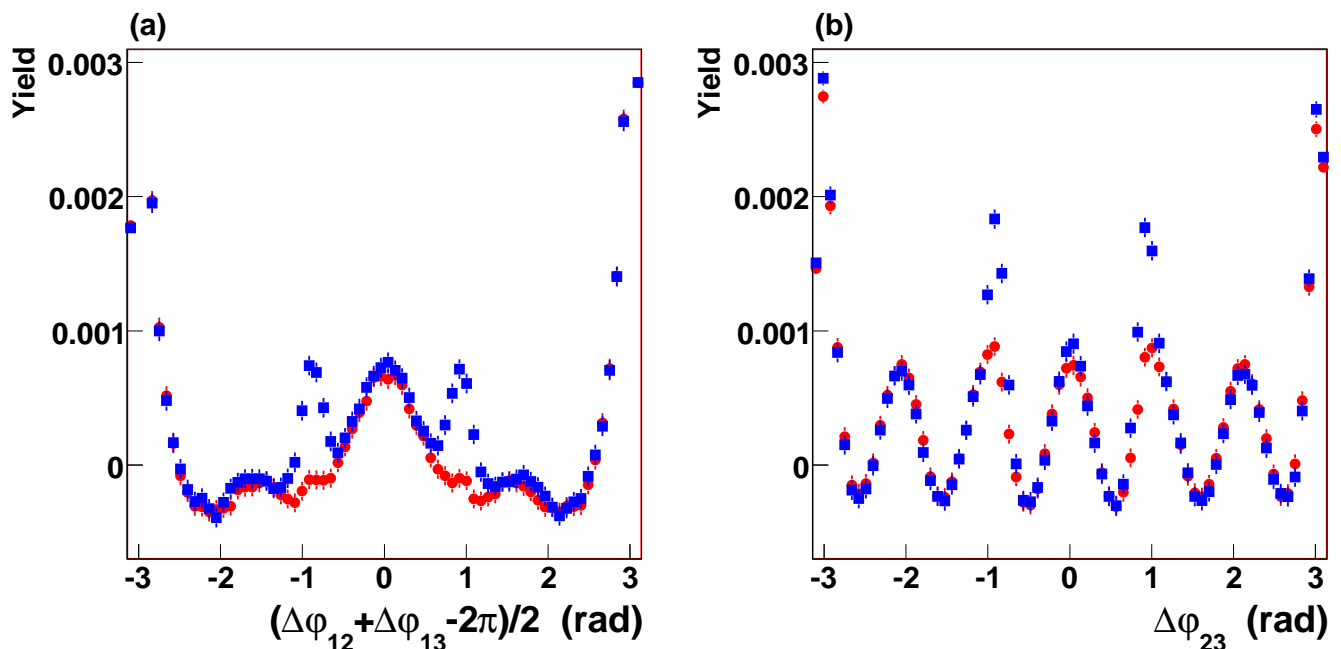


FIG. 11: (Color online) Comparison of the cone signal obtained with an average of two (blue squares) and one (red circles) low- p_t particles involved in conical emission. Panel (a) and (b) show the 3-cumulant projections along $(\Delta\varphi_{12} + \Delta\varphi_{13})/2$ and $\Delta\varphi_{23}$ respectively. Simulations carried out with a jet-flow component, $v_2 = 0.05$, and an average number of 100 low- p_t background particles per event, with flow $v_2 = 0.1$, and $v_4 = v_2^2$. See text for details.

VII. SUMMARY AND CONCLUSIONS

Conical emission has been suggested in the recent literature to explain the away-side structures observed in two particle azimuthal correlations for $Au + Au$ collisions at $\sqrt{s_{NN}} = 200$ GeV. If realized, conical emission should also lead to three particle correlations. We introduced in Ref. [41] a method based on cumulants to carry a search for such a signal. In this work, we presented a discussion of the properties of the three particle cumulant (3-cumulant) calculated in terms of two relative azimuthal angles, as defined in [41], for searches of conical emission in high-energy $A + A$ collisions. We showed that in the presence of azimuthal anisotropy (flow), the 3-cumulant reduces to non-diagonal terms dominated by components of order $v_2 v_2 v_4$ for Poissonian particle production. Given particle production is in

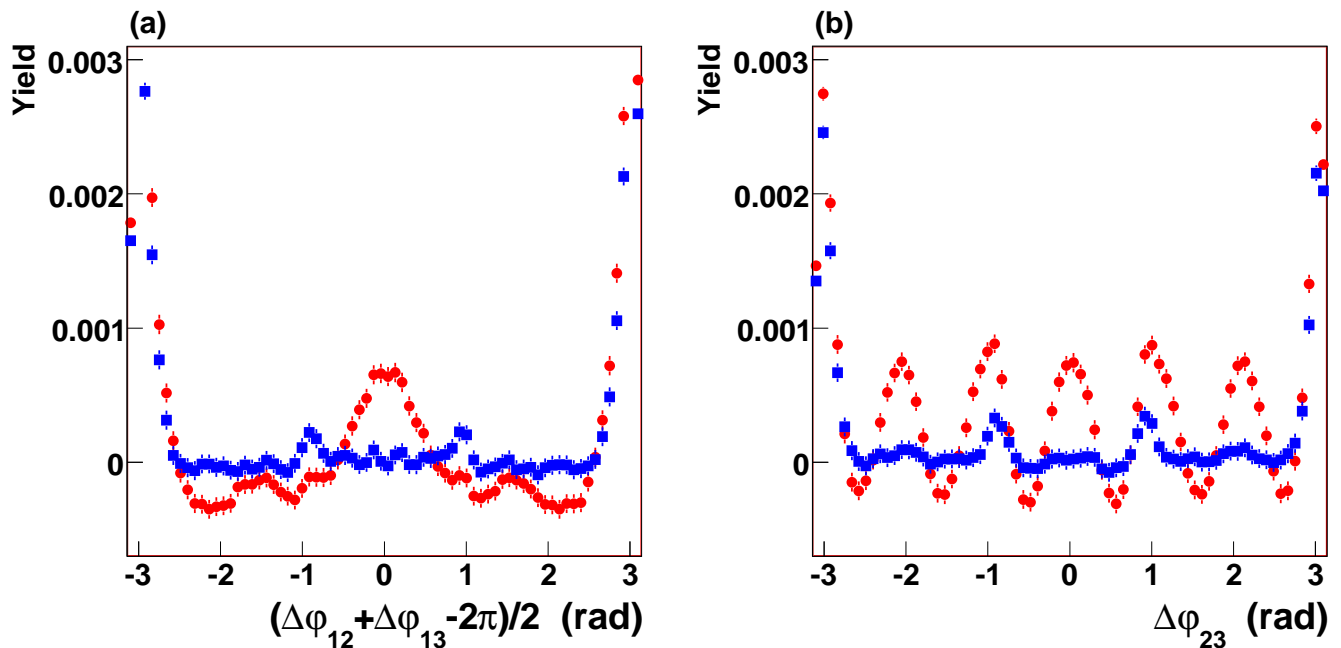


FIG. 12: (Color online) Comparison of the cone signal obtained with an average of one low- p_t particles involved in conical emission and an average of 100 low- p_t background particles per event with $v_2 = 0.05$ (red circles) and $v_2 = 0.1$ (blue squares). Panel (a) and (b) show the 3-cumulant projections along $(\Delta\varphi_{12} + \Delta\varphi_{13})/2$ and $\Delta\varphi_{23}$ respectively. Simulations are carried out with a jet-flow component, $v_2 = 0.05$. The background has $v_4 = v_2^2$.

general non-Poissonian, one however expects the presence of second order terms, dominated by components in v_2^2 in the cumulant. The strength of those terms relative to the irreducible $v_2 v_2 v_4$ components depends on the magnitude of v_2 and the global strength of particle correlations, or departure from Poisson statistics. The strength of particle correlation is known to vary inversely with the collision multiplicity in $A + A$ collisions due to increasing two-particle correlation dilution with increasing number of collision participants. We thus expect the mix of $v_2 v_2 v_4$ and v_2^2 should be a function of collision centrality.

We introduced a three-particle probability cumulant, and showed it is devoid of v_2^2 non-Poissonian components in the presence of flow only thereby enabling, in principle, the determination of $v_2 v_2 v_4$ amplitudes. We discussed the shape and strength of the 3-cumulant based on simple particle production models including di-jets, mono-jet plus conical emission, and jet \times flow correlations. We showed that jet \times flow cross-terms should be more complex than those assumed by some ongoing analyses, and cannot, in particular, be derived from a product of two-particle flow and jet-like terms. We used the models to discuss the sensitivity of the 3-cumulant for searches of conical emission in $A + A$ collisions. We showed that the cumulant enables excellent sensitivity to conical emission for modest values of flow v_2 , but becomes increasingly challenging for larger values of v_2 . We further showed that conical emission can be detected even in the presence of jet \times flow correlations for small values of v_2 jet flow. It is however obvious the signal may be masked by large values of jet and background v_2 and large non-Poissonian particle production. Precise values of sensitivity, in terms of signal strength to background ratios, cannot be expressed in a model independent way, and are found to depend on the relative amplitude of background v_2 and v_4 jet-flow correlations, as well as the global strength of particle correlations, i.e. departure from Poisson statistics.

This work neglects effects associated with momentum conservation, quantum number conservation, and particle correlations present in $p+p$ collisions. Momentum conservation implies in particular that a multicomponent description of particle production is not strictly valid, and while it is useful to estimate the effects of various particle production mechanisms, its use to search for conical emission signals is model dependent and therefore unreliable.

Acknowledgements

The author thanks S. Voloshin, M. Sharma, and A. Poskanzer for their critical reading of the manuscript, valuable comments and discussions. This work was supported in part by DOE Grant No. DE-FG02-92ER40713.

References

-
- [1] J. Hoffmann, H. Stoecker, U. Heinz, W. Scheid, and W. Greiner, Phys. Rev. Lett. **36**, 88 (1976).
- [2] H. Stoecker, Nucl. Phys. **A750**, 121 (2005).
- [3] J. Ruppert, J. Phys. Conf. Ser. **27**, 217 (2005).
- [4] J. Casalderrey-Solana, E. V. Shuryak, and D. Teaney, J. Phys. Conf. Ser. **27**, 22 (2005).
- [5] J. Ruppert, B. Mller, Physics Letters **B618**, 123 (2005).
- [6] T. Renk and J. Ruppert, Phys. Rev. C **73**, 011901 (2006).
- [7] A. K. Chaudhuri, U. W. Heinz, Phys. Rev. Lett. **97**, 062301 (2006).
- [8] H. Stoecker, *et al.* nucl-th/0703054, 2007.
- [9] T. Renk, J. Ruppert, hep-ph/0702102.
- [10] B. Muller, J. of Physics G: Nucl. Part. Phys. (QM 08 Proceedings) in press.
- [11] B. Betz, J. of Physics G: Nucl. Part. Phys. (QM 08 Proceedings) in press.
- [12] S. Mukherjee, M. Mustafa, and F. Ray, Phys. Rev. D **75**, 094015 (2007).
- [13] S. Gubser, S. Pufu, and A. Yarom, Phys. Rev. Lett. **100** 012301. (2008).
- [14] I.M. Dremin, JETP Lett. **30** 140 (1979).
- [15] I.M. Dremin, Sov. J. Nucl. Phys. **33** 726 (1981).
- [16] I.M. Dremin, Nucl. Phys. A **767**, 233 (2006).
- [17] V. Koch, A. Majumber, X.-N. Wang, Phys. Rev. Lett. **96**, 172302 (2005).
- [18] A. Majumder, B. Muller, S. A. Bass (2006), hep-ph/0611135.
- [19] I. Vitev, Phys. Lett. B **630**, 78 (2005).
- [20] A.D. Polosa and C.A. Salgado, hep-ph/0607295.
- [21] C. B. Chiu, R. C. Hwa, Phys. Rev. C **74**, 064909 (2006).
- [22] N. Armesto, *et al.*, Phys. Rev. Lett. **93**, 242301 (2004), hep-ph/0405301.
- [23] N. Armesto, C.A. Salgado, U. A. Wiedemann, Phys. Rev. C **72**, 064910 (2005).
- [24] T. Renk and J. Ruppert, Phys. Lett. **B646**, 19 (2007).
- [25] T. Renk and J. Ruppert, Phys. Rev. C **76**, 014908 (2007).
- [26] S.A. Voloshin, Phys. Lett. B **632**, 490 (2006) arXiv:nucl-th/0312065.
- [27] C. B. Chiu, R. C. Hwa, Phys. Rev. C **72**, 034903 (2005), nucl-th/0505014.
- [28] W. G. Holzmann, N. N. Ajitanand, J. M. Alexander, P. Chung, M. Issah, R. A. Lacey, A. Taranenko and A. Shevel, J. Phys. Conf. Ser. **27**, 80 (2005).
- [29] Chun Zhang *et al.* (PHENIX Collaboration), J. of Physics G: Nucl. Part. Phys. **34**, S671 (2007).
- [30] J. Ulery, *et al.* (STAR Collaboration), Nucl. Phys. A **774**, 581 (2006).
- [31] J. Ulery and F. Wang, nucl-ex/0609016.
- [32] J. Ulery, *et al.* (STAR Collaboration), nucl-ex/07040224.
- [33] J. Ulery, Ph.D. Thesis, Purdue University, (2007).
- [34] N.N. Ajitanand (PHENIX Collaboration), Nucl. Phys. **A774** 585 (2006).
- [35] J. Ulery, *et al.* (STAR Collaboration), Nucl. Phys. A **783**, 511 (2007).
- [36] Stefan Kniege and Mateusz Ploskon, *et al.* (CERES Collaboration), J. of Physics G: Nucl. Part. Phys. **34**, S697 (2007).
- [37] S. Kniege, M. Ploskon (CERES Collaboration), nucl-ex/0703008.
- [38] N. N. Ajitanand, Nucl. Phys. **A783** 519 (2007).
- [39] N. Borghini, Phys.Rev. C **75** (2007) 021904.
- [40] Zbigniew Chajeccki, and Mike Lisa, arXiv:0807.3569.
- [41] C. A. Pruneau, Phys. Rev. C **74** 064910 (2006).
- [42] C. Pruneau, *et al.* (STAR Collaboration), J. of Physics G: Nucl. Part. Phys. **34**, S667 (2007).
- [43] E. L. Berger, Nucl. Phys. **B85**, 61 (1975)..
- [44] P. Carruthers and I. Sarcevic, Phys. Rev. Lett. **63**, 1561 (1989).
- [45] M. Anderson *et al.* (STAR Collaboration), Nucl. Instrum. Meth. **A 499** 659 (2003).
- [46] STAR Collaboration, private communication.
- [47] T. Affolder, *et al.* STAR Collaboration, Phys. Rev. D **65**, 092002 (2002).
- [48] I. Arsene *et al.* BRAHMS Collaboration, Nucl. Phys. A **757**, 1 (2005); K. Adcox *et al.* PHENIX Collaboration, *ibid.* . 184; B. B. Back *et al.* PHOBOS Collaboration, *ibid.* . 28; J. Adams *et al.* STAR Collaboration, *ibid.* . 102.
- [49] J. Adams *et al.* STAR Collaboration, Phys. Rev. C **72**, 014904 (2005).
- [50] S. A. Voloshin, A. M. Poskanzer, and R. Snelling, nucl-ex/0809.2949.
- [51] N. N. Ajitanand, *et al.* Phys.Rev. C **72**, 011902(2005).
- [52] M. Horner, *et al.* (STAR Collaboration), J. of Physics G: Nucl. Part. Phys. **34**, S995 (2007).